

Variable Coordination Mode of Chloranilic Acid. Synthesis, Structure, and Electrochemical Properties of Some Osmium Complexes

Parna Gupta,[†] Anindya Das,[†] Falguni Basuli,[†] Alfonso Castineiras,[‡] William S. Sheldrick,[§] Heike Mayer-Figge,[§] and Samaresh Bhattacharya^{*†}

Department of Chemistry, Inorganic Chemistry Section, Jadavpur University, Kolkata 700 032, India, Departamento de Química Inorganica, Universidade de Santiago de Compostela, Campus Universitario Sur, E-15706 Santiago de Compostela, Spain, and Lehrstuhl Fur Analytische Chemie, Ruhr Universitat Bochum, D-44780 Bochum, Germany

Received June 30, 2004

Reaction of chloranilic acid (H_2ca) with $[Os(bpy)_2Br_2]$ ($bpy = 2,2'$ -bipyridine) affords a dinuclear complex of type $[Os(bpy)_2]_2(ca)]^{2+}$, isolated as the perchlorate salt. A similar reaction of H_2ca with $[Os(PPh_3)_2(pap)Br_2]$ ($pap = 2$ -(phenylazo)pyridine) affords a dinuclear complex of type $[Os(PPh_3)_2(pap)]_2(ca)]^{2+}$ (isolated as the perchlorate salt) and a mononuclear complex of type $[Os(PPh_3)_2(pap)(ca)]$. Reaction of H_2ca with $[Os(PPh_3)_2(CO)_2(HCOO)_2]$ gives a dinuclear complex of type $[Os(PPh_3)_2(CO)_2]_2(r-ca)]$, where $r-ca$ is the two electron reduced form of the chloranilate ligand. The structures of the $[Os(PPh_3)_2(pap)]_2(ca)](ClO_4)_2$, $[Os(PPh_3)_2(pap)(ca)]$, and $[Os(PPh_3)_2(CO)_2]_2(r-ca)]$ complexes have been determined by X-ray crystallography. In the $[Os(bpy)_2]_2(ca)]^{2+}$ and $[Os(PPh_3)_2(pap)]_2(ca)]^{2+}$ complexes, the chloranilate dianion is serving as a tetradentate bridging ligand. In the $[Os(PPh_3)_2(pap)(ca)]$ complex, the chloranilate dianion is serving as a bidentate chelating ligand. In the $[Os(PPh_3)_2(CO)_2]_2(r-ca)]$ complex, the reduced form of the chloranilate ligand ($r-ca^{4-}$) is serving as a tetradentate bridging ligand. All the four complexes are diamagnetic and show intense metal-to-ligand charge-transfer transitions in the visible region. The $[Os(PPh_3)_2(pap)(ca)]$ complex shows an $Os(II)–Os(III)$ oxidation, followed by an $Os(III)–Os(IV)$ oxidation on the positive side of a standard calomel electrode. The three dinuclear complexes show two successive oxidations on the positive side of SCE. The mixed-valent $Os^{II}–Os^{III}$ species have been generated in the case of the two chloranilate-bridged complexes by coulometric oxidation of the homovalent $Os^{II}–Os^{II}$ species. The mixed-valent $Os^{II}–Os^{III}$ species show intense intervalence charge-transfer transitions in the near-IR region.

Introduction

There has been significant current interest toward the synthesis of polynuclear complexes of the transition-metal ions, largely because of the interesting spectroscopic, magnetic, catalytic, and redox properties exhibited by such complexes.¹ The most interesting aspect in the study of the chemistry of such multinuclear complexes is the degree of communication between the different metal centers. All the three basic components of the polynuclear assemblies, viz., the metal ions, the bridging ligands, and the terminal ligands, contribute to the quality of the metal–metal interaction. To assess the influence of these three basic components on the

degree of communication between the metal centers, there have been numerous studies on dinuclear transition-metal complexes.² The main objective of most of these studies has been to chemically control the metal–metal communication in the dinuclear complexes by planned variation of one or more of the three basic components. The present study was also initiated with a similar target, viz., to find out the effect of the peripheral ligands on the degree of metal–metal interaction in a group of diosmium complexes. The bridging ligand picked up for this study is chloranilic acid (H_2ca , **1**). Though this ligand has an extensive coordination chemistry, which has recently been reviewed,³ it is particularly famous as an efficient bridging ligand through which metal–metal communication is known to take place effectively. We were particularly interested to synthesize diosmium complexes bridged by the chloranilate dianion (**2**). As chloranilic acid

* Author to whom correspondence should be addressed. E-mail: samaresh_b@hotmail.com.

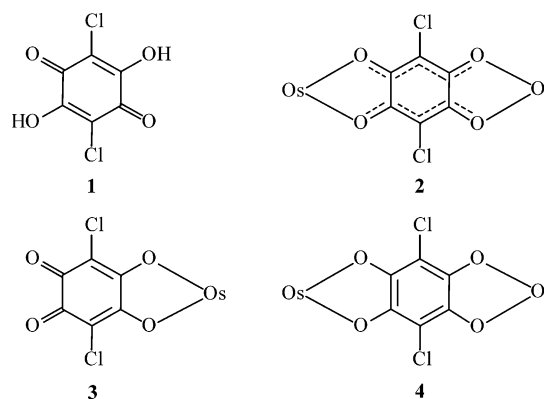
[†] Jadavpur University.

[‡] Universidade de Santiago de Compostela.

[§] Ruhr Universitat Bochum.

has close resemblance with the dioxolelene ligands, which are known to have π levels of comparable energy with the metal d orbitals,⁴ interesting electrochemical properties were expected from the targeted complexes. It may be mentioned here that, though few ruthenium complexes of chloranilic acid (and 2,5-dihydroxy-1,4-benzoquinone) are known,⁵ there is no report on any osmium chloranilate complex in the literature. Realizing that successful synthesis of such osmium complexes containing **2** would require osmium complexes containing two labile ligands that are mutually cis, three such osmium complexes, viz., $[\text{Os}(\text{bpy})_2\text{Br}_2]$ (bpy = 2,2'-bipyridine),⁶ $[\text{Os}(\text{PPh}_3)_2(\text{pap})\text{Br}_2]$ (pap = 2-phenylazo)pyridine,⁷ and $[\text{Os}(\text{PPh}_3)_2(\text{CO})_2(\text{HCOO})_2]$,⁸ were utilized as osmium starting materials. Reaction of chloranilic acid with these osmium starting materials indeed afforded diosmium complexes containing **2**, in addition to complexes of other types where the chloranilate dianion served as a

bidentate O,O-donor (**3**) as well as a rather unexpected coordination mode **4**, in which a reduced form of the chloranilate dianion bridges two osmium centers. The chemistry of all these complexes is reported in this paper with special reference to their synthesis, structure, and redox properties.



- (1) (a) Lu, X.-X.; Li, C.-K.; Cheng, E. C.-C.; Zhu, N.; Yam, V. W.-W. *Inorg. Chem.* **2004**, *43*, 2225. (b) Teixeira, L. J.; Seabra, M.; Reis, E.; Giraio da Cruz, M. T.; Pedrosa de Lima, M. C.; Pereira, E.; Miranda, M. A.; Marques, M. P. M. *J. Med. Chem.* **2004**, *47*, 2917. (c) Canada-Vilalta, C.; Streib, W. E.; Huffman, J. C.; O'Brien, T. A.; Davidson, E. R.; Christou, G. *Inorg. Chem.* **2004**, *43*, 101. (d) Escuer, A.; Fallah, M. S. E.; Vicente, R.; Sanz, N.; Font-Bardia, M.; Solans, X.; Mautner, F. A. *J. Chem. Soc., Dalton Trans.* **2004**, 1867. (e) Xie, Y.-B.; Zhang, C.; Li, J.-R.; Bu, X.-H. *J. Chem. Soc., Dalton Trans.* **2004**, 562. (f) Li, J.-R.; Bu, X.-H.; Zhang, R. H. *J. Chem. Soc., Dalton Trans.* **2004**, 813. (g) Wheate, N. J.; Day, A. I.; Blanch, R. J.; Arnold, A. P.; Cullinane, C.; Collins, J. G. *Chem. Commun.* **2004**, 1424. (h) Polson, M. I. J.; Hanan, G. S.; Taylor, N. J.; Hasenkopf, B.; Thouvenot, R. *Chem. Commun.* **2004**, 1314. (i) Hofmeier, H.; Elghayoury, A.; Schenning, A. P. H. J.; Schubert, U. S. *Chem. Commun.* **2004**, 318. (j) Kanamori, K. *Coord. Chem. Rev.* **2003**, *237*, 147. (k) Wheate, N. J.; Collins, J. G. *Coord. Chem. Rev.* **2003**, *241*, 133. (l) Tu, C.; Lin, J.; Shao, Y.; Guo, Z. *Inorg. Chem.* **2003**, *42*, 5795. (m) Alonso, E.; Fornies, J.; Fortunato, C.; Martin, A.; Orpen, A. G. *Organometallics* **2003**, *22*, 5011. (n) Visser, C.; van den Hende, J. R.; Meetsma, A.; Hessen, B. *Organometallics* **2003**, *22*, 615. (o) Umakoshi, K.; Yamauchi, Y.; Nakamiya, K.; Kojima, T.; Yamasaki, M.; Kawano, H.; Onishi, M. *Inorg. Chem.* **2003**, *42*, 3907. (p) Thompson, M. K.; Lough, A. J.; White, A. J. P.; Williams, D. J.; Kahwa, I. A. *Inorg. Chem.* **2003**, *42*, 4828. (q) Yip, J. H. K.; Wu, J.; Wong, K.-Y.; Yeung, K.-W.; Vittal, J. J. *Organometallics* **2002**, *21*, 612. (r) Michon, C.; Djukic, J.-P.; Ratkovic, Z.; Collin, J.-P.; Pfeffer, M.; de Cian, A.; Fischer, J.; Heiser, D.; Dotz, K. H.; Nieger, M. *Organometallics* **2002**, *21*, 3519. (s) Pavlishchuk, V.; Birkelbach, F.; Weyhermuller, T.; Wieghardt, K.; Chaudhuri, P. *Inorg. Chem.* **2002**, *41*, 4405. (t) Sun, S. S.; Lees A. J. *Coord. Chem. Rev.* **2002**, *230*, 170.
- (2) (a) Serroni, S.; Campagna, S.; Puntoriero, F.; Pietro, C. D.; McClenaghan, N. D.; Loiseau, F. *Chem. Soc. Rev.* **2001**, 367. (b) Launay, J.-P. *Chem. Soc. Rev.* **2001**, 386. (c) Ward, M. D. *Chem. Soc. Rev.* **1995**, 121. (d) Giuffrida, G.; Campagna, S. *Coord. Chem. Rev.* **1994**, *135*–136, 517.
- (3) Kitagawa, S.; Kawata, S. *Coord. Chem. Rev.* **2002**, *224*, 11.
- (4) (a) da Silva, R. S.; Gorelsky, S. I.; Dodsworth, E. S.; Tfouni, E.; Lever, A. B. P. *J. Chem. Soc., Dalton Trans.* **2000**, 4078. (b) Auburn, P. R.; Dodsworth, E. S.; Haga, M.; Liu, W.; Nevin, W. A.; Lever, A. B. P. *Inorg. Chem.* **1991**, *30*, 3502. (c) Masui, H.; Lever, A. B. P.; Auburn, P. R. *Inorg. Chem.* **1991**, *30*, 2402. (d) Haga, M.; Dodsworth, E. S.; Lever, A. B. P. *Inorg. Chem.* **1986**, *25*, 447.
- (5) (a) Jasimuddin, S.; Byabartta, P.; Sinha, C.; Mostafa, G.; Lu, T. H. *Inorg. Chim. Acta* **2004**, *357*, 2015. (b) Ando, I.; Saeki, N.; Hamaghi, T.; Ujimoto, K.; Kurihara, H. *Fukuoka Daigaku Rigaku Shuho* **2002**, *32*, 13. (c) Gupta, A. K.; Gupta, A.; Choudhury, A. *Ind. J. Chem.* **2002**, *41A*, 2076. (d) Gupta, A. K.; Poddar, R. K.; Choudhury, A. *Ind. J. Chem.* **2000**, *39A*, 1191. (e) Ward, M. D. *Inorg. Chem.* **1996**, *35*, 1712.
- (6) Kober, E. M.; Casper, J. V.; Sullivan, B. P.; Meyer, T. J. *Inorg. Chem.* **1988**, *27*, 4587.
- (7) Das, A.; Peng, S. M.; Bhattacharya, S. *Polyhedron* **2000**, *19*, 1227.
- (8) Gupta, P.; Basuli, F.; Peng, S. M.; Lee, G. H.; Bhattacharya, S. *Ind. J. Chem.* **2003**, *42A*, 2406.

Experimental Section

Materials. Commercial osmium tetroxide was purchased from Arora Matthey, Kolkata, India, and was converted into $[\text{NH}_4]_2[\text{OsBr}_6]$ by reduction with hydrobromic acid.⁹ $[\text{Os}(\text{PPh}_3)_3\text{Br}_2]$ was synthesized from $[\text{NH}_4]_2[\text{OsBr}_6]$, following a reported procedure. $[\text{Os}(\text{bpy})_2\text{Br}_2]$, $[\text{Os}(\text{PPh}_3)_2(\text{pap})\text{Br}_2]$, and $[\text{Os}(\text{PPh}_3)_2(\text{CO})_2(\text{HCOO})_2]$ were prepared according to the reported procedures.^{6–8} Chloranilic acid (H_2ca) was purchased from Loba Chemie, Mumbai, India. All other chemicals and solvents were reagent grade commercial materials and were used as received.

Preparations of Complexes. $[\{\text{Os}(\text{bpy})_2\}_2(\text{ca})](\text{ClO}_4)_2$. To a solution of chloranilic acid (15 mg, 0.07 mmol) and triethylamine (15 mg, 0.15 mmol) in 3:1 2-methoxyethanol–water (50 mL) was added $[\text{Os}(\text{bpy})_2\text{Br}_2]$ (100 mg, 0.15 mmol). The resulting solution was heated at reflux for 24 h to produce a deep-blue solution. The solution was cooled to room temperature, and a saturated aqueous solution of NaClO_4 (0.5 mL) was added to it. $[\{\text{Os}(\text{bpy})_2\}_2(\text{ca})](\text{ClO}_4)_2$ slowly precipitated as a dark-brown solid, which was collected by filtration, washed with water, and dried in vacuo over P_4O_{10} (**Warning!** Perchlorate salts are potentially explosive and hence should be handled with care.). Yield: 68%. Anal. Calcd: C, 39.15; H, 2.27; N, 7.94. Found: C, 39.17; H, 2.25; N, 7.95. Mass spectrometry (MS) (fast-atom bombardment (FAB), *m*-nitrobenzyl alcohol): $m/z = 1275 (M^+ - \text{ClO}_4 - \text{Cl})$, $1177 (M^+ - 2\text{ClO}_4 - \text{Cl})$. $\Lambda_M = 240 \Omega^{-1} \text{cm}^2 \text{M}^{-1}$ in acetonitrile solution. Diamagnetic.

$[\{\text{Os}(\text{PPh}_3)_2(\text{pap})\}_2(\text{ca})](\text{ClO}_4)_2$. $[\text{Os}(\text{PPh}_3)_2(\text{pap})\text{Br}_2]$ (106 mg, 0.10 mmol) and chloranilic acid (10 mg, 0.05 mmol) were dissolved in dichloromethane (10 mL), and to this solution was added ethanol (30 mL) and triethylamine (10 mg, 0.10 mmol). The mixture was heated at reflux for 48 h affording a brown solution. After being cooled to room temperature, a saturated aqueous solution of NaClO_4 (0.5 mL) was added to it. $[\{\text{Os}(\text{PPh}_3)_2(\text{pap})\}_2(\text{ca})](\text{ClO}_4)_2$ separated as a green crystalline solid, which was collected by filtration, and the filtrate was preserved for further processing (see below). The green residue was washed with ice-cold water and dried in vacuo over P_4O_{10} . Yield: 22%. Anal. Calcd: C, 54.55; H, 3.55; N, 3.82. Found: C, 54.53; H, 3.56; N, 3.84. MS (FAB, *m*-nitrobenzyl alcohol): $m/z = 1740 (M^+ - \text{PPh}_3)$, $1478 (M^+ - 2\text{PPh}_3)$, 1216

(9) Hoffman, P. R.; Caulton, K. G. *J. Am. Chem. Soc.* **1975**, *97*, 4221.

Table 1. Crystallographic Data for $[\{\text{Os}(\text{PPh}_3)_2(\text{pap})\}_2(\text{ca})](\text{ClO}_4)_2$, $[\text{Os}(\text{PPh}_3)_2(\text{pap})(\text{ca})]$, and $[\{\text{Os}(\text{PPh}_3)_2(\text{CO})_2\}_2(\text{r-ca})]$

empirical formula	$\text{C}_{106}\text{H}_{84}\text{Cl}_4\text{N}_6\text{O}_{12}\text{P}_4\text{Os}_2$	$\text{C}_{53}\text{H}_{41}\text{Cl}_2\text{N}_3\text{O}_5\text{P}_2\text{Os}$	$\text{C}_{82}\text{H}_{60}\text{Cl}_4\text{O}_8\text{P}_4\text{Os}_2$
fw	2279.87	1122.93	1748.48
space group	Triclinic, $P\bar{1}$	Monoclinic, $P2_1/c$	Triclinic, $P\bar{1}$
a , Å	12.1895(9)	17.6020(17)	10.302(3)
b , Å	12.8575(11)	13.2730(15)	12.262(3)
c , Å	17.0049(13)	25.176(3)	15.481(5)
α , deg	88.500(10)	90	99.96(2)
β , deg	80.518(9)	127.15(10)	105.47(3)
γ , deg	70.631(9)	90	104.69(4)
V , Å ³	2478.8(3)	4688.3(9)	1761.4(9)
Z	1	4	2
λ , Å	0.71073	0.71073	0.71073
cryst size, mm ³	0.25 × 0.15 × 0.10	0.30 × 0.30 × 0.05	0.29 × 0.24 × 0.15
T , K	173(2)	208(2)	293(2)
μ , mm ⁻¹	2.797	2.955	3.829
$R1^a$	0.0457	0.0391	0.0437
wR2 ^b	0.1284	0.0794	0.0926
GOF ^c	1.058	0.996	1.023

^a $R1 = \sum |F_o| - |F_c| / \sum |F_o|$. ^b $wR2 = [\sum [w(F_o^2 - F_c^2)^2] / \sum [w(F_o^2)^2]]^{1/2}$. ^c $GOF = [\sum [w(F_o^2 - F_c^2)^2] / (M - N)]^{1/2}$, where M is the number of reflections and N is the number of parameters refined.

($M^+ - 3\text{PPh}_3$). $\Lambda_M = 230 \Omega^{-1} \text{ cm}^2 \text{ M}^{-1}$ in acetonitrile solution. Diamagnetic.

[Os(PPh₃)₂(pap)(ca)]. The red filtrate obtained from the above reaction was evaporated to dryness under reduced pressure and the solid mass, thus obtained, was subjected to purification by thin-layer chromatography on a silica plate. Using 1:1 benzene-acetonitrile as the eluant a red band separated, which was extracted with acetonitrile. Evaporation of the extract afforded [Os(PPh₃)₂(pap)(ca)] as a red crystalline solid. Yield: 46%. Anal. Calcd C, 57.61; H, 3.53; N, 3.80. Found: C, 57.40; H, 3.55; N, 3.81. MS (FAB, *m*-nitrobenzyl alcohol): $m/z = 1107(M^+)$, 844 ($M^+ - \text{PPh}_3$), 636 ($M^+ - \text{PPh}_3 - \text{ca}$), 456 ($M^+ - \text{PPh}_3 - \text{ca-pap}$). Diamagnetic.

[{Os(PPh₃)₂(CO)₂}₂(r-ca)]. To a solution of chloranilic acid (12 mg, 0.06 mmol) in 2-methoxyethanol (40 mL) was added [Os(PPh₃)₂(CO)₂(HCOO)₂] (50 mg, 0.12 mmol). The resultant solution was refluxed for 24 h. Partial evaporation of this solution afforded [{Os(PPh₃)₂(CO)₂}₂(r-ca)] as a blue microcrystalline solid, which was collected by filtration, washed with cold ethanol, and dried in air. Yield: 70%. Anal. Calcd: C, 50.56; H, 3.08. Found: C, 50.80; H, 3.47. MS (FAB, *m*-nitrobenzyl alcohol): $m/z = 1749(M^+)$, 1486 ($M^+ - \text{PPh}_3$), 1224 ($M^+ - 2\text{PPh}_3$). Diamagnetic.

Physical Measurements. Microanalyses (C, H, N) were performed using a Heraeus Carlo Erba 1108 elemental analyzer. The FAB mass spectra were recorded on a JEOL SX 102/DA-6000 mass spectrometer/data system using Argon/Xenon (6 kV, 10 mA) as the FAB gas. Magnetic susceptibilities were measured using a PAR 155 vibrating sample magnetometer fitted with a Walker Scientific L75FBAL magnet. IR spectra were obtained on a Perkin-Elmer 783 spectrometer with samples prepared as KBr pellets. Solution electrical conductivities were measured using a Phillips PR 9500 bridge with a solute concentration of 10^{-3} M. Electronic spectra were recorded on a JASCO V-570 spectrophotometer. Electrochemical measurements were made using a CH Instruments model 600A electrochemical analyzer. A platinum disk working electrode, a platinum wire auxiliary electrode, and an aqueous saturated calomel reference electrode (SCE) were used in the cyclic voltammetry experiments. A platinum-wire gauge-working electrode was used in the coulometric experiments. Electronic spectra of the coulometrically oxidized solutions were recorded after placing the solutions in a spectrophotometric cell and then transferring them quickly to the spectrophotometer. All electrochemical experiments were performed under a dinitrogen atmosphere. All electrochemical data were collected at 298 K and are uncorrected for junction potentials.

Crystallography of [{Os(PPh₃)₂(pap)}₂(ca)](ClO₄)₂. Single crystals of [{Os(PPh₃)₂(pap)}₂(ca)](ClO₄)₂ were obtained by slow diffusion of benzene into a dichloromethane solution of the complex. Selected crystal data and data collection parameters are given in Table 1. Data were collected on a Stoe IPDS diffractometer using graphite-monochromated Mo K α radiation ($\lambda = 0.71073$ Å) by ω scans within the θ range $3.22 < \theta < 29.06^\circ$. X-ray data reduction, structure solution, and refinement were done using the SHELXS-97 and SHELXL-97 packages.¹⁰ The structure was solved by the direct methods.

Crystallography of [Os(PPh₃)₂(pap)(ca)]. Single crystals of [Os(PPh₃)₂(pap)(ca)] were obtained by slow evaporation of a solution of the complex in 1:1 ethanol-acetone. Selected crystal data and data collection parameters are given in Table 1. Data were collected on an Enraf Nonius CAD4 automatic diffractometer using graphite monochromated Mo K α radiation ($\lambda = 0.71073$ Å) by ω scans within the θ range $3.06 < \theta < 25.96^\circ$. X-ray data reduction and structure solution and refinement were done as stated above.

Crystallography of [{Os(PPh₃)₂(CO)}₂(r-ca)]. Single crystals of [{Os(PPh₃)₂(CO)}₂(r-ca)] were obtained directly from the synthetic reaction in 2-methoxyethanol. Selected crystal data and data collection parameters are given in Table 1. Data were collected on a Siemens P4 diffractometer using graphite-monochromated Mo K α radiation ($\lambda = 0.71073$ Å) using ω scans within the angular range $1.96 < \theta < 23.50^\circ$. X-ray data reduction and structure solution and refinement were done as stated above.

Results and Discussion

A. Reaction with [Os(bpy)₂Br₂]. Reaction of chloranilic acid was first carried out with [Os(bpy)₂Br₂] in a 1:2 molar ratio, which gave the expected diosmium complex, viz., [{Os(bpy)₂}₂(ca)]²⁺. The complex cation was isolated as perchlorate salt in a decent yield. Microanalytical, mass spectral, magnetic susceptibility, and conductance data of this [{Os(bpy)₂}₂(ca)](ClO₄)₂ complex have confirmed its composition. As both 2,2'-bipyridine and the chloranilate dianion are symmetric ligands, the [{Os(bpy)₂}₂(ca)]²⁺ complex is assumed to have a symmetric structure (5). Structural characterization of this complex by X-ray crystal-

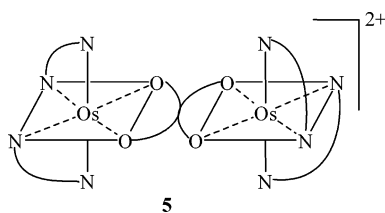
(10) SHELXS-97 and SHELXL-97 Sheldrick, G. M. *SHELXS-97 and SHELXL-97*; Fortran programs for crystal structure solution and refinement: University of Göttingen, Germany, 1997.

Table 2. Electronic Spectral and Cyclic Voltammetric Data

compound	electronic spectral data λ_{\max} , nm (ϵ , $M^{-1} \text{ cm}^{-1}$)	cyclic voltammetric data ^c $E_{\text{pa}}, E_{\text{pc}}$ V vs SCE
$[\{\text{Os}(\text{bpy})_2\}_2(\text{ca})](\text{ClO}_4)_2^a$	1 242 (11 500), 882 (26 000), 758 ^f (21 800), 518 (16 400), 424 ^f (15 800), 340 (20 700)	0.76 (60) ^e , 0.33 (60) ^e , −1.11 (60) ^e , −1.79 (90) ^e , −2.17 (140) ^e
$[\{\text{Os}(\text{PPh}_3)_2(\text{pap})\}_2(\text{ca})](\text{ClO}_4)_2^a$	1 394 ^f (2 800), 1 064 (4 900), 754 ^f (20 700), 682 (28 500), 334 (40 800), 276 ^f (44 600)	1.53 (70) ^e , 1.22 (100) ^e , −0.76 ^g , −0.90 ^g , −1.22 ^g
$[\text{Os}(\text{PPh}_3)_2(\text{pap})(\text{ca})]^a$	1 060 ^f (400), 728 ^f (600), 550 ^f (7 600), 516 (11 000), 422 ^f (7 700), 338 (13 000), 274 (19 200)	1.72 ^h , 0.88 (70) ^e , −0.92 ^g , −1.33 ^g
$[\{\text{Os}(\text{PPh}_3)_2(\text{CO})_2\}_2(\text{r-ca})]^b$	806 (6 000) ^f , 614 (13 000), 380 (10 000), 306 (18 000) ^f , 276 (3 300) ^f	1.43 (77) ^e , 1.95 ^h

^a In acetonitrile. ^b In 1:9 dichloromethane–acetonitrile. ^c Supporting electrolyte, TBAP; scan rate, 50 mV s^{-1} . ^d $E_{1/2} = 0.5(E_{\text{pa}} + E_{\text{pc}})$, where E_{pa} and E_{pc} are anodic and cathodic peak potential. ^e $\Delta E_{\text{p}} = E_{\text{pa}} - E_{\text{pc}}$ (mV). ^f Shoulder. ^g E_{pc} value. ^h E_{pa} value.

lography has not been possible, as its crystals could not be grown. The IR spectrum of $[\{\text{Os}(\text{bpy})_2\}_2(\text{ca})](\text{ClO}_4)_2$ shows



sharp bands at 1473, 1418, 1254, 1018, 764, 721, and 665 cm^{-1} , which are also found in the spectrum of $[\text{Os}(\text{bpy})_2\text{Br}_2]$, and hence these are attributed to the $\text{Os}(\text{bpy})_2$ fragment. Three additional bands at 1493, 1090, and 623 cm^{-1} are displayed by $[\{\text{Os}(\text{bpy})_2\}_2(\text{ca})](\text{ClO}_4)_2$, of which the band at 1493 cm^{-1} is assigned to the $\nu_{\text{C-O}}$ stretch of the coordinated chloranilate ligand,⁴ and the other two bands at 1090 and 623 cm^{-1} are due to the perchlorate ion. Electronic spectrum of $[\{\text{Os}(\text{bpy})_2\}_2(\text{ca})](\text{ClO}_4)_2$, recorded in acetonitrile solution, shows several intense absorptions in the UV, visible, and near-IR regions (Table 2, Figure 1). The absorptions in the UV region are attributable to transitions within the ligand orbitals, while those in the near-IR and visible regions are probably due to metal-to-ligand charge-transfer (MLCT) transitions. Multiple charge-transfer transitions in such mixed-ligand complexes are very common, and they usually result from the lower symmetry splitting of the metal level, the presence of different acceptor orbitals, and from the mixing of singlet and triplet configurations in the excited state through spin–orbit coupling.¹¹

Electrochemical properties of $[\{\text{Os}(\text{bpy})_2\}_2(\text{ca})](\text{ClO}_4)_2$ have been studied by cyclic voltammetry in acetonitrile solution (0.1 M TBAP). Voltammetric data are given in Table 2, and the voltammogram is shown in Figure 2. Two successive oxidative responses are displayed by this complex at 0.33 and 0.76 V.¹² As both osmium(II) and the chloranilate dianion (ca^{2-}) can potentially undergo oxidation, and the frontier molecular orbitals in such species usually have

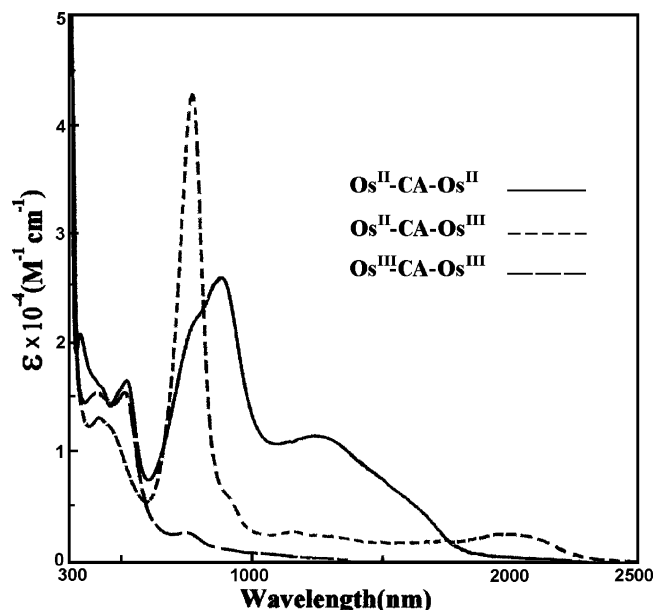


Figure 1. Electronic spectra of $[\{\text{Os}^{\text{II}}(\text{bpy})_2\}_2(\text{ca})](\text{ClO}_4)_2$ (solid line), $[(\text{bpy})_2\text{Os}^{\text{III}}(\text{ca})\text{Os}^{\text{II}}(\text{bpy})_2]^{3+}$ (dotted line) and $[\{\text{Os}^{\text{III}}(\text{bpy})_2\}_2(\text{ca})]^{4+}$ (dashed line) in acetonitrile solution.

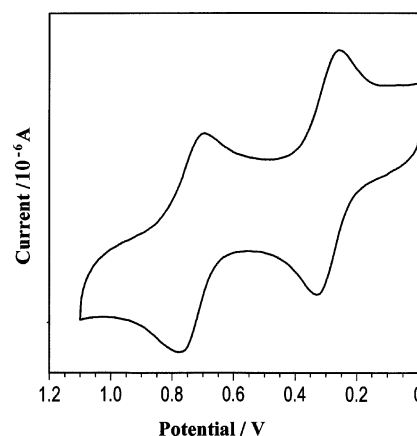


Figure 2. Cyclic voltammogram of $[\{\text{Os}^{\text{II}}(\text{bpy})_2\}_2(\text{ca})](\text{ClO}_4)_2$ in acetonitrile solution (0.1 M TBAP) at a scan rate of 50 mV s^{-1} .

- (11) (a) Kober, E. M.; Meyer, T. J. *Inorg. Chem.* **1982**, *21*, 3967. (b) Ceulemans, A.; Vanquickenborne, L. G. *J. Am. Chem. Soc.* **1981**, *103*, 2238. (c) Decuritus, S.; Felix, F.; Ferguson, J.; Gudel, H. U.; Ludi, A. *J. Am. Chem. Soc.* **1980**, *103*, 4102. (d) Pankuch, B. J.; Lacky, D. E.; Crosby, G. A. *J. Phys. Chem.* **1980**, *84*, 2061.

(12) All potentials are referenced to SCE.

substantial ligand(ca) character,^{5c} assignment of specific site of oxidation is rather difficult. However, in view of the assignments of similar responses in the analogous ruthenium complex,^{5c} these responses are assigned to the successive Os(II)–Os(III) oxidations. It may be relevant to note that

mononuclear osmium(II) complexes of type $[\text{Os}(\text{bpy})_2(\text{O}-\text{O})]^+$ (where O–O represents a monoanionic bidentate O,O donor ligand) have been observed to display Os(II)–Os(III) oxidation at similar potentials.¹³ Both the responses are reversible, characterized by a peak-to-peak separation (ΔE_p) of 60 mV, and the anodic peak current (i_{pa}) is almost equal to the cathodic peak current (i_{pc}), as expected for a reversible electron-transfer process. The one-electron nature of both the oxidations has been verified by comparing their current heights (i_{pa}) with that of the standard ferrocene/ferrocenium couple under identical experimental conditions. The fairly large separation (430 mV) between these two couples shows that the two metal centers can communicate effectively through this bridging ligand (ca^{2-}). The observed separation of potentials corresponds to a comproportionation constant¹⁴ $K_c = 1.85 \times 10^7$ for the $[(\text{bpy})_2\text{Os}^{\text{III}}(\text{ca})\text{Os}^{\text{II}}(\text{bpy})_2]^{3+}$ complex, the magnitude of which indicates that the mixed-valent complex should be fairly stable. $[\{\text{Os}(\text{bpy})_2\}_2(\text{ca})](\text{ClO}_4)_2$ also shows three reductive responses at -1.11 , -1.79 , and -2.17 V. In view of the fact that the chloranilate dianion (ca^{2-}) can undergo facile two-electron reduction to generate the corresponding tetra-anion (r-ca^{4-} , vide infra), the first two responses are assigned to successive reductions of the coordinated chloranilate ligand.³ The third response is assigned to reduction of the coordinated bpy ligand.¹⁵

The electrochemical reversibility of the Os(II)–Os(III) couples indicates that the partially oxidized $[(\text{bpy})_2\text{Os}^{\text{III}}(\text{ca})\text{Os}^{\text{II}}(\text{bpy})_2]^{3+}$ and fully oxidized $[\{\text{Os}^{\text{III}}(\text{bpy})_2\}_2(\text{ca})]^{4+}$ species are stable on the cyclic voltammetric time scale. The relatively low potentials of these oxidations suggest that the oxidized complexes may also be stable on longer time scales. To investigate this, the $[\{\text{Os}^{\text{II}}(\text{bpy})_2\}_2(\text{ca})]^{2+}$ complex has been coulometrically oxidized first at 0.45 V in acetonitrile solution (0.1 M TBAP). The oxidation was smooth and quantitative and was accompanied by a color change of brown to green. The green solution containing the oxidized $[(\text{bpy})_2\text{Os}^{\text{III}}(\text{ca})\text{Os}^{\text{II}}(\text{bpy})_2]^{3+}$ complex shows similar cyclic voltammetric responses to its precursor $[\{\text{Os}^{\text{II}}(\text{bpy})_2\}_2(\text{ca})]^{2+}$ complex, except that the first couple near 0.3 V now appears as a reductive response. The electronic spectrum of the partially oxidized $[(\text{bpy})_2\text{Os}^{\text{III}}(\text{ca})\text{Os}^{\text{II}}(\text{bpy})_2]^{3+}$ complex shows (Figure 1, Table 4), in addition to intense absorptions in the near-IR and visible regions, a distinctly new absorption at 2028 nm, which is assigned to intervalence charge-transfer (IVCT) transition. The green solution containing the partially oxidized $[\text{Os}^{\text{III}}(\text{bpy})_2(\text{ca})\text{Os}^{\text{II}}(\text{bpy})_2]^{3+}$ complex has been further oxidized coulometrically at 0.95 V. The oxidation has again been quantitative and the green solution gradually turned brownish-violet. Cyclic voltammetry on the brownish-violet solution confirms the generation of the fully oxidized $[\{\text{Os}^{\text{III}}(\text{bpy})_2\}_2(\text{ca})]^{4+}$ complex. The electronic spectrum of

Table 3. Selected Bond Distances and Bond Angles for $[\{\text{Os}(\text{PPh}_3)_2(\text{pap})\}_2(\text{ca})](\text{ClO}_4)_2$, $[\text{Os}(\text{PPh}_3)_2(\text{pap})(\text{ca})]$, and $[\{\text{Os}(\text{PPh}_3)_2(\text{CO})_2\}_2(\text{r-ca})]$

$[\{\text{Os}(\text{PPh}_3)_2(\text{pap})\}_2(\text{ca})](\text{ClO}_4)_2$			
bond distances (Å)			
Os(1)–N(11)	2.045(4)	O(1)–C(1)	1.281(6)
Os(1)–N(13)	1.983(4)	O(2)–C(3)	1.276(6)
Os(1)–O(1)	2.118(4)	N(12)–N(13)	1.298(6)
Os(1)–O(2)#1	2.111(4)	C(1)–C(2)	1.393(7)
Os(1)–P(1)	2.4216(13)	C(1)–C(3a)	1.502(7)
Os(1)–P(2)	2.4349(13)	C(2)–C(3)	1.401(7)
bond angles (deg)			
P(1)–Os(1)–P(2)	177.09(5)	N(11)–Os(1)–N(13)	76.06(18)
N(11)–Os(1)–O(2)#1	178.49(14)	N(13)–Os(1)–O(1)	175.56(16)
O(1)–Os(1)–O(2)#1	75.25(14)		
$[\text{Os}(\text{PPh}_3)_2(\text{pap})(\text{ca})]$			
bond distances (Å)			
Os(1)–N(11)	2.001(5)	C(6)–O(4)	1.218(7)
Os(1)–N(13)	1.951(5)	N(12)–N(13)	1.349(7)
Os(1)–O(1)	2.081(5)	C(1)–C(2)	1.361(8)
Os(1)–O(2)	2.117(4)	C(2)–C(3)	1.500(7)
Os(1)–P(1)	2.4224(15)	C(3)–C(4)	1.380(8)
Os(1)–P(2)	2.4083(14)	C(4)–C(5)	1.408(8)
O(1)–C(2)	1.300(6)	C(5)–C(6)	1.561(9)
O(2)–C(3)	1.288(7)	C(6)–C(1)	1.430(8)
C(5)–O(3)	1.224(7)		
bond angles (deg)			
P(1)–Os(1)–P(2)	175.01(5)	N(11)–Os(1)–O(2)	173.51(18)
O(1)–Os(1)–O(2)	76.57(14)	N(13)–Os(1)–O(1)	175.19(19)
N(11)–Os(1)–N(13)	76.7(2)		
$[\{\text{Os}(\text{PPh}_3)_2(\text{CO})_2\}_2(\text{r-ca})]$			
bond distances (Å)			
Os(1)–C(1)	1.806(15)	C(2)–O(21)	1.184(11)
Os(1)–C(2)	1.863(11)	O(1)–C(4)	1.302(8)
Os(1)–O(1)	2.115(5)	O(2)–C(3)	1.310(9)
Os(1)–O(2)	2.105(5)	C(3)–C(4)	1.447(11)
Os(1)–P(1)	2.394(2)	C(3)–C(5)	1.394(10)
Os(1)–P(4)	2.234(2)	C(5)–C(4#1)	1.399(10)
C(1)–O(11)	1.186(15)		
bond angles (deg)			
P(1)–Os(1)–P(4)	175.32(9)	O(11)–C(1)–Os(1)	178.5(15)
C(1)–Os(1)–O(1)	172.7(5)	O(21)–C(2)–Os(1)	179.1(10)
O(1)–Os(1)–O(2)	77.5(2)		

this fully oxidized $[\{\text{Os}^{\text{III}}(\text{bpy})_2\}_2(\text{ca})]^{4+}$ complex shows (Figure 1, Table 4) the disappearance of the IVCT band displayed at 2028 nm by the partially oxidized species.

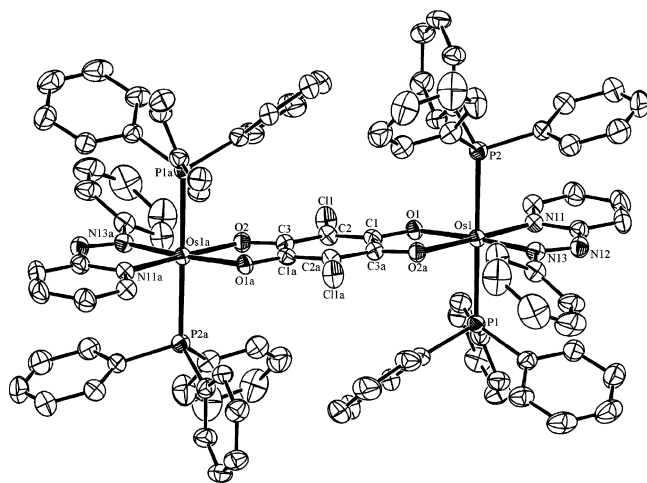
B. Reaction with $[\text{Os}(\text{PPh}_3)_2(\text{pap})\text{Br}_2]$. Facile formation of the chloranilate bridged diosmium complex, $[\{\text{Os}(\text{bpy})_2\}_2(\text{ca})]^{2+}$, via displacement of the bromides from *cis*- $[\text{Os}(\text{bpy})_2\text{Br}_2]$, encouraged us to explore the possibility of synthesizing such diosmium complexes utilizing other osmium starting materials containing a *cis*-OsBr₂ fragment. Thus we selected $[\text{Os}(\text{PPh}_3)_2(\text{pap})\text{Br}_2]$ (pap = 2-(phenylazo)pyridine), which also has a *cis*-OsBr₂ fragment, as the next starting material.⁷ The coordinated bromides in this complex have also been observed to be displaceable by chelating bidentate ligands under relatively mild conditions.⁷ With the hope of obtaining a diosmium complex as before, reaction of chloranilic acid has been carried out with $[\text{Os}(\text{PPh}_3)_2(\text{pap})\text{Br}_2]$ in the presence of triethylamine. A mixture of two complexes, a green complex and a red complex, has been obtained from this reaction. The combined yield of these complexes has been satisfactory. Characterization of these two complexes is separately described below.

- (13) (a) Basuli, F.; Peng, S. M.; Bhattacharya, S. *Polyhedron* **1998**, *17*, 2191. (b) Haga, M. A.; Isobe, K.; Boone, S. R.; Pierpont, C. G. *Inorg. Chem.* **1990**, *29*, 3795. (c) Sullivan, B. P.; Casper, J. V.; Johnson, S. R.; Meyer, T. J. *Organometallics* **1984**, *3*, 1241.
- (14) Laye, R. H.; Couchman, S. M.; Ward, M. D. *Inorg. Chem.* **2001**, *40*, 4089.
- (15) (a) Basuli, F.; Peng, S. M.; Bhattacharya, S. *Inorg. Chem.* **2000**, *39*, 1120. (b) Del Medico, A.; Dodsworth, E. S.; Auburn, P. R.; Pietro, W. J.; Lever, A. B. P. *Inorg. Chem.* **1994**, *33*, 1583.

Table 4. Electronic Spectral Data of the Coulometrically Generated Species

compound	electronic spectral data ^a λ_{\max} , nm (ϵ , M ⁻¹ cm ⁻¹)
$[(\text{bpy})_2\text{Os}^{\text{III}}(\text{ca})\text{Os}^{\text{II}}(\text{bpy})_2]^{3+}$	2 028 (2 500), 1 164 (2 600), 926 ^b (5 300), 766 (42 900), 470 ^b (11 700), 414 (13 000)
$[\{\text{Os}^{\text{III}}(\text{bpy})_2\}_2(\text{ca})]^{4+}$	750 ^c (2 500), 510 (15 400), 442 ^b (14 700), 406 (15 400)
$[(\text{PPh}_3)_2(\text{pap})\text{Os}^{\text{III}}(\text{ca})\text{Os}^{\text{II}}(\text{PPh}_3)_2(\text{pap})]^{3+}$	1 750 ^b (1 500), 1 112 (3 300), 686 ^b (7 300), 612 (9 200), 492 ^b (6 100), 334 ^b (17 900), 222 (42 200)

^a Acetonitrile solution. ^b Shoulder.

**Figure 3.** View of the $[\{\text{Os}(\text{PPh}_3)_2(\text{pap})\}_2(\text{ca})]^{2+}$ complex.

The Green Complex. Preliminary characterization (microanalytical, mass spectral, magnetic susceptibility, and conductance) data of the green complex have been found to be consistent with the expected formulation, viz., $[\{\text{Os}(\text{PPh}_3)_2(\text{pap})\}_2(\text{ca})](\text{ClO}_4)_2$. To verify the coordination mode of chloranilic acid in this complex, as well as to find out the stereochemistry of the complex, its structure has been determined by X-ray crystallography. The structure is shown in Figure 3, and relevant bond parameters are given in Table 3. The structure shows that the chloranilate dianion is indeed coordinated to the two osmium centers in the expected bridging mode (2). Two PPh_3 and a pap are also coordinated to each osmium center. The pyridyl-azo fragments of the coordinated pap ligands are sharing the same equatorial plane with the chloranilate ligand and the metal ions, while the phenyl ring of each pap is slightly away from this plane. The two PPh_3 ligands linked to each osmium are mutually trans. The $\text{N}_2\text{O}_2\text{P}_2$ coordination sphere around each osmium is distorted from ideal octahedral geometry, as reflected in the bond parameters around osmium. The Os–N, Os–O, and Os–P distances are quite normal.⁷ The C–O and C–C distances within the coordinated chloranilate ligand are consistent with the charge delocalization possible in this dianionic tetradentate ligand.³

IR spectrum of $[\{\text{Os}(\text{PPh}_3)_2(\text{pap})\}_2(\text{ca})](\text{ClO}_4)_2$ shows strong bands at 1088 and 627 cm^{-1} for ClO_4^- and 519, 694, and 745 cm^{-1} due to the PPh_3 ligands. The $\nu_{\text{C}=\text{O}}$ stretch of the chloranilate ligand is observed as a sharp band at 1494 cm^{-1} , and a strong band at 1312 cm^{-1} is attributable to the $\nu_{\text{N}=\text{N}}$ stretch of the pap ligand.⁷ Electronic spectrum of $[\{\text{Os}(\text{PPh}_3)_2(\text{pap})\}_2(\text{ca})](\text{ClO}_4)_2$, recorded in acetonitrile solution,

shows several intense absorptions in the UV, visible, and near-IR regions (Table 2). As before, the absorptions in the UV region are assigned to transitions within the ligand orbitals and those in the near-IR and visible regions are believed to be due to MLCT ($t_2-\pi^*$ of pap and ca) charge-transfer transitions.

Cyclic voltammetry on $[\{\text{Os}(\text{PPh}_3)_2(\text{pap})\}_2(\text{ca})](\text{ClO}_4)_2$ in acetonitrile solution (0.1 M TBAP) shows two oxidative responses at 1.22 and 1.53 V (Table 2). As the bridging chloranilate dianion (ca^{2-}) in $[\{\text{Os}(\text{bpy})_2\}_2(\text{ca})](\text{ClO}_4)_2$ did not show any oxidation in this region, the observed oxidative responses are tentatively assigned to successive Os(II)–Os(III) oxidations. Though the peak currents (i_{pa} and i_{pc}) for the first oxidation are almost equal, the peak-to-peak separation (ΔE_{p}) is slightly higher than that expected for an ideally reversible response, probably due to kinetic reasons. The second one is close to the solvent cutoff and appears to be irreversible. The separation between the two oxidations is relatively small (310 mV) compared to that observed in the $[\{\text{Os}(\text{bpy})_2\}_2(\text{ca})](\text{ClO}_4)_2$ complex. Irreversibility of the second oxidation vitiates evaluation of a meaningful disproportionation constant. However, the smaller separation itself shows that in this $[\{\text{Os}(\text{PPh}_3)_2(\text{pap})\}_2(\text{ca})](\text{ClO}_4)_2$ complex the two metal centers communicate less effectively through the same bridging ligand, and the observed difference in metal–metal communication is attributable to the difference in the nature of the terminal ligands. The nearly reversible nature of the first Os(II)–Os(III) couple indicates that the partially oxidized $[(\text{PPh}_3)_2(\text{pap})\text{Os}^{\text{III}}(\text{ca})\text{Os}^{\text{II}}(\text{PPh}_3)_2(\text{pap})]^{3+}$ complex may probably be generated in solution. Hence the $[\{\text{Os}(\text{PPh}_3)_2(\text{pap})\}_2(\text{ca})]^{2+}$ complex has been coulometrically oxidized at 1.30 V in acetonitrile solution (0.1 M TBAP). The oxidation has been quantitative, associated with a color change of green to blue. The electronic spectrum of this partially oxidized $[(\text{PPh}_3)_2(\text{pap})\text{Os}^{\text{III}}(\text{ca})\text{Os}^{\text{II}}(\text{PPh}_3)_2(\text{pap})]^{3+}$ complex shows an IVCT transition at 1750 nm, in addition to intense absorptions in the near-IR and visible regions (Table 4). Three reductive responses are displayed by $[\{\text{Os}(\text{PPh}_3)_2(\text{pap})\}_2(\text{ca})](\text{ClO}_4)_2$ at -0.76 , -0.90 , and -1.22 V, of which the second one is assigned to reduction of the coordinated chloranilate ligand and the first and third ones are assigned to reductions of the coordinated pap ligands.⁷

The Red Complex. Preliminary characterization (microanalytical, mass spectral, and magnetic susceptibility) data of the red complex are found to correspond well to a mononuclear neutral complex having the $[\text{Os}(\text{PPh}_3)_2(\text{pap})-(\text{ca})]$ composition, which again indicates that the chloranilate

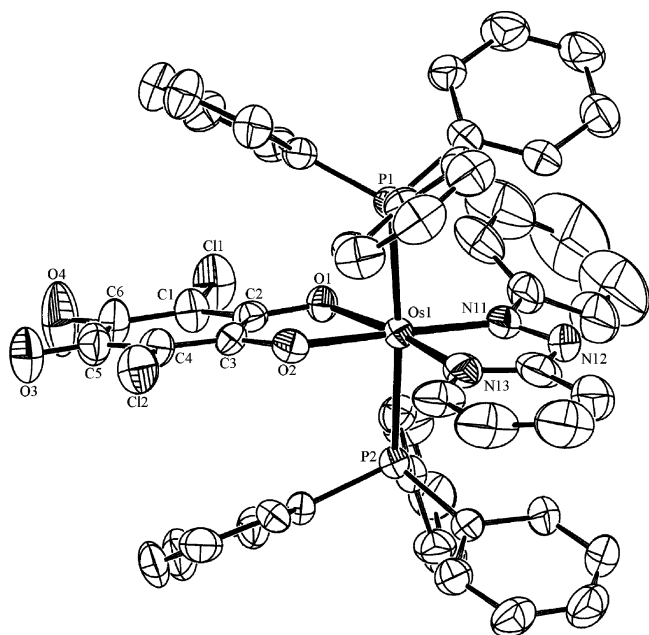


Figure 4. View of the $[\text{Os}(\text{PPh}_3)_2(\text{pap})(\text{ca})]$ complex.

ligand is probably bound to the metal center as a dianionic bidentate chelating ligand (**3**) in this complex. To verify the coordination mode of the chloranilate ligand, the structure of this red complex has been determined by X-ray crystallography. The structure is shown in Figure 4, and some selected bond parameters are listed in Table 3. The structure shows that this red complex is indeed a mononuclear complex having the expected composition, where the chloranilate ion is coordinated to the metal center in the expected fashion (**3**). The stereochemistry is distorted octahedral, where the coordinated pap and the chloranilate ligand have constituted one equatorial plane with the metal at the center and the PPh_3 ligands have occupied the remaining two axial positions. The bond distances within the $\text{Os}(\text{PPh}_3)_2(\text{pap})$ fragment (Table 3) are comparable to those observed in the same fragment of the green $\{[\text{Os}(\text{PPh}_3)_2(\text{pap})]_2(\text{ca})\}(\text{ClO}_4)_2$ complex (vide supra). The C–O and C–C distances within the coordinated coordinated chloranilate ligand are consistent with the charge description in **3**.^{3,5a}

The IR spectrum of $[\text{Os}(\text{PPh}_3)_2(\text{pap})(\text{ca})]$ shows bands due to the coordinated PPh_3 ligands (at 518, 696, and 745 cm^{-1}) and the $\nu_{\text{N}=\text{N}}$ stretch of the pap ligand (at 1316 cm^{-1}). The $\nu_{\text{C}=\text{O}}$ stretch of the chloranilate ligand is observed at 1089 cm^{-1} and another sharp band at 1526 cm^{-1} attributable to the $\nu_{\text{C}=\text{O}}$ stretch of the chloranilate ligand.³ The electronic spectrum of $[\text{Os}(\text{PPh}_3)_2(\text{pap})(\text{ca})]$, recorded in acetonitrile solution, shows several intense absorptions in the UV, visible, and near-IR region (Table 2). Cyclic voltammetry on $[\text{Os}(\text{PPh}_3)_2(\text{pap})_2(\text{ca})]$ in acetonitrile solution (0.1 M TBAP) shows two oxidative responses (Table 2). On the basis of the E_L parameters of the coordinated ligands,^{5a,16} the first reversible response at 0.88 V is assigned to $\text{Os}(\text{II})\text{--Os}(\text{III})$ oxidation. The second oxidation at 1.72 V is irreversible and is tentatively assigned to the $\text{Os}(\text{III})\text{--Os}(\text{IV})$ oxidation. Two reductive responses are displayed by $[\text{Os}(\text{PPh}_3)_2(\text{pap})(\text{ca})]$

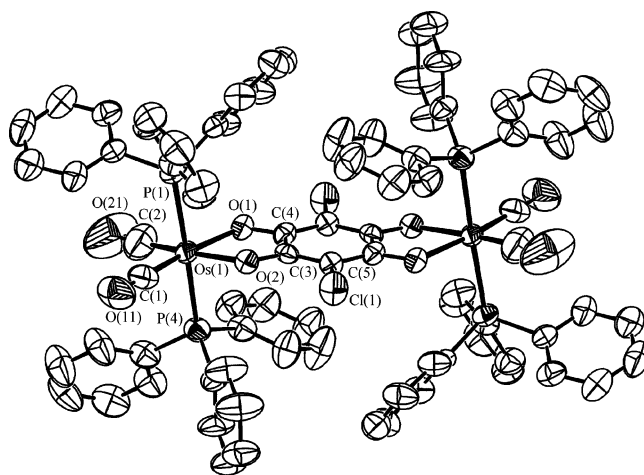


Figure 5. View of the $\{[\text{Os}(\text{PPh}_3)_2(\text{CO})_2]_2(\text{r-ca})\}$ complex.

at -0.92 , and -1.33 V , which are assigned to reductions of the coordinated pap ligands.

C. Reaction with $[\text{Os}(\text{PPh}_3)_2(\text{CO})_2(\text{HCOO})_2]$. Reaction of chloranilic acid has been finally carried out with another osmium starting material, viz., $[\text{Os}(\text{PPh}_3)_2(\text{CO})_2(\text{HCOO})_2]$, where the coordinated formates are found to be easily replaceable by bidentate chelating ligands.⁸ The reaction proceeds smoothly in refluxing 2-methoxyethanol to afford a blue complex. Though the preliminary characterization data (microanalysis, mass spectral, etc.) gave indications that in this blue complex two $\text{Os}(\text{PPh}_3)_2(\text{CO})_2$ fragments are bridged by a ligand having similar composition as the chloranilate ligand, there was ambiguity regarding specific charge distribution in this complex. The identity of this blue complex has been unveiled by its structure determination by X-ray crystallography. The structure is shown in Figure 5, and some selected bond parameters are listed in Table 3. The structure shows that two $\text{Os}(\text{PPh}_3)_2(\text{CO})_2$ fragments are indeed bridged by a ligand, which has a skeletal similarity with the chloranilate ion. However, a closer look at the bond distances within the bridging ligand reveals that the chloranilic acid has not only undergone deprotonation upon complexation but also has undergone a two-electron reduction during the course of the synthetic reaction. All four C–O lengths are significantly longer than those observed in the $\{[\text{Os}(\text{PPh}_3)_2(\text{pap})]_2(\text{ca})\}^{2+}$ complex, and the C–C lengths are also consistent with a fully aromatic phenyl ring. This complex may therefore be formulated as $\{[\text{Os}(\text{PPh}_3)_2(\text{CO})_2]_2(\text{r-ca})\}$, where r-ca represents the reduced tetranionic chloranilate ligand (**4**). Bond lengths in the $\text{Os}(\text{PPh}_3)_2(\text{CO})_2$ fragments compare well with those observed in structurally characterized complexes of osmium(II) containing the same fragment.⁸ While the exact mechanism of the observed redox reaction is not completely clear to us, it appears that the reducing equivalent may be provided by the displaced formates.

The IR spectrum of $\{[\text{Os}(\text{PPh}_3)_2(\text{CO})_2]_2(\text{r-ca})\}$ shows strong bands at 2031 and 1963 cm^{-1} due to the coordinated CO ligands. Strong bands are also observed at 516 , 695 , and 748 cm^{-1} , due to the coordinated PPh_3 ligands. Comparison with the spectrum of $[\text{Os}(\text{PPh}_3)_2(\text{CO})_2(\text{HCOO})_2]$ shows that some new bands (at 1497 , 1408 , and 1094) are present in

(16) Lever, A. B. P. *Inorg. Chem.* **1990**, *29*, 1271.

the spectrum of the $[\{\text{Os}(\text{PPh}_3)_2(\text{CO})_2\}_2(\text{r-ca})]$ complex, which must be due to the coordinated r-ca ligand. The band at 1094 cm^{-1} is attributable to the $\nu_{\text{C-O}}$ stretch of the r-ca⁴⁻ ligand.³ Electronic spectrum of $[\{\text{Os}(\text{PPh}_3)_2(\text{CO})_2\}_2(\text{r-ca})]$, recorded in dichloromethane solution, show several intense MLCT transitions in the visible and near-IR regions (Table 2). Cyclic voltammetry on $[\{\text{Os}(\text{PPh}_3)_2(\text{CO})_2\}_2(\text{r-ca})]$ in 1:9 dichloromethane–acetonitrile solution¹⁷ (0.1 M TBAP) shows two oxidative responses at 1.43 and 1.95 V (Table 2). As the oxidations occur at fairly high potentials, and both the metal center as well as the reduced chloranilate (r-ca⁴⁻) ligand can undergo oxidation at such potentials, assignment of the oxidative responses has not been possible. The first oxidation is quasi-reversible ($\Delta E_p = 77\text{ mV}$ and $i_{\text{pa}} > i_{\text{pc}}$), while the second oxidation is irreversible.

Conclusions

The present study shows that chloranilic acid (H₂ca) can display different modes of coordination in its complexes, which is manifested in its reaction with $[\text{Os}(\text{bpy})_2\text{Br}_2]$, $[\text{Os}(\text{PPh}_3)_2(\text{pap})\text{Br}_2]$, and $[\text{Os}(\text{PPh}_3)_2(\text{CO})_2(\text{HCOO})_2]$. The present study also shows that the degree of metal–metal com-

munication in the chloranilate(ca²⁻)-bridged diosmium complexes is considerably influenced by the nature of the terminal ligands. Studies on chloranilate(ca²⁻)-bridged dinuclear complexes of several other metal ions are in progress. The nature of the two unutilized oxygens in the mononuclear $[\text{Os}(\text{PPh}_3)_2(\text{pap})(\text{ca})]$ complex indicates the possibility of using it as a building unit for the construction of polynuclear assemblies. Such a possibility is currently under exploration.

Acknowledgment. The authors thank the RSIC at Central Drug Research Institute, Lucknow, India, for the C, H, and N analysis data. A.D. and P.G. thank the Council of Scientific and Industrial Research, New Delhi, for their fellowship (Grant Nos. 9/96(415)/2003/EMR-I and 9/96(325)/2000/EMR-I, respectively). The authors thank the reviewers for their critical comments and constructive suggestions, which have been helpful in preparing the revised version.

Supporting Information Available: Figures showing the electronic spectra of $[\{\text{Os}(\text{PPh}_3)_2(\text{pap})\}_2(\text{ca})](\text{ClO}_4)_2$, $[(\text{PPh}_3)_2(\text{pap})\text{Os}^{\text{III}}(\text{ca})\text{Os}^{\text{II}}(\text{PPh}_3)_2(\text{pap})]^{3+}$, $[\text{Os}(\text{PPh}_3)_2(\text{pap})(\text{ca})]$, and $[\{\text{Os}(\text{PPh}_3)_2(\text{CO})_2\}_2(\text{r-ca})]$, cyclic voltammograms of $[\{\text{Os}(\text{PPh}_3)_2(\text{pap})\}_2(\text{ca})](\text{ClO}_4)_2$, $[\text{Os}(\text{PPh}_3)_2(\text{pap})(\text{ca})]$, and $[\{\text{Os}(\text{PPh}_3)_2(\text{CO})_2\}_2(\text{r-ca})]$, and X-ray crystallographic data in CIF format. This material is available free of charge via the Internet at <http://pubs.acs.org>.

IC049149S

(17) A little dichloromethane was necessary to take the complex into solution. Addition of large excess of acetonitrile was necessary to record the redox responses in proper shape.